

Polymorphic phase transformations of 3-chloro-*trans*-cinnamic acid and its solid solution with 3-bromo-*trans*-cinnamic acid

Manal A. Khoj,[‡] Colan E. Hughes and Kenneth D. M. Harris*

School of Chemistry, Cardiff University, Main Building, Park Place, Cardiff CF10 3AT, UK. *Correspondence e-mail: harriskdm@cardiff.ac.uk

Received 11 May 2018

Accepted 26 June 2018

Edited by M. Kubicki, Adam Mickiewicz University, Poland

[‡] Current address: Chemistry, Umm Al-Qura University, Makkah, Saudi Arabia

Keywords: cinnamic acid; polymorph; phase transformation; crystal structure; solid solution.

CCDC references: 1828662; 1828663

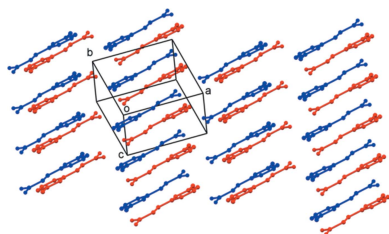
Supporting information: this article has supporting information at journals.iucr.org/c

We have investigated the polymorphic phase transformations above ambient temperature for 3-chloro-*trans*-cinnamic acid (3-ClCA, C₉H₇ClO₂) and a solid solution of 3-ClCA and 3-bromo-*trans*-cinnamic acid (3-BrCA, C₉H₇BrO₂). At 413 K, the γ polymorph of 3-ClCA transforms to the β polymorph. Interestingly, the structure of the β polymorph of 3-ClCA obtained in this transformation is different from the structure of the β polymorph of 3-BrCA obtained in the corresponding polymorphic transformation from the γ polymorph of 3-BrCA, even though the γ polymorphs of 3-ClCA and 3-BrCA are isostructural. We also report a high-temperature phase transformation from a γ -type structure to a β -type structure for a solid solution of 3-ClCA and 3-BrCA (with a molar ratio close to 1:1). The γ polymorph of the solid solution is isostructural with the γ polymorphs of pure 3-ClCA and pure 3-BrCA, while the β -type structure produced in the phase transformation is structurally similar to the β polymorph of pure 3-BrCA.

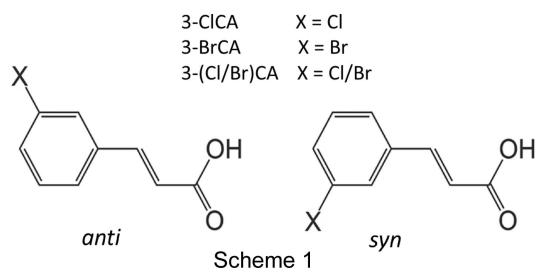
1. Introduction

trans-Cinnamic acid and its derivatives have been central to the development of organic solid-state chemistry, particularly with regard to polymorphism and the demonstration that well-defined structure–reactivity relationships exist for the different polymorphs, which was central to the development of the topochemical principle (Kohlschütter & Tüscher, 1920; Cohen *et al.*, 1964; Cohen & Schmidt, 1964; Cohen, 1964, 1975; Hirshfield & Schmidt, 1964; Schmidt, 1964, 1967, 1971; Thomas, 1974, 1979; Nakanishi *et al.*, 1981; Hasegawa, 1986; Enkelmann *et al.*, 1993; Harris *et al.*, 1991; Guo *et al.*, 2008). Crystalline *trans*-cinnamic acids can be classified into three types (denoted α , β and γ) based on their photochemical behaviour in [2 + 2] photodimerization reactions (Mustafa, 1952; Cohen *et al.*, 1964). The α -type and β -type crystals are photoreactive (the distance between the centres of the C=C bonds of potentially reactive monomer molecules is less than *ca* 4.2 Å), whereas the γ -type crystals are photostable (the distance between the centres of adjacent C=C bonds is more than *ca* 4.7 Å). The difference between the photoreactive α -type and β -type crystals concerns the geometric relationship between potentially reactive monomer molecules. In α -type structures, potentially reactive molecules are related across an inversion centre, which leads to a centrosymmetric dimer molecule upon photodimerization. In β -type structures, potentially reactive molecules are instead related by translation, which leads to a mirror-symmetric dimer molecule upon photodimerization.

In this article, we focus on 3-chloro-*trans*-cinnamic acid (3-ClCA) and 3-bromo-*trans*-cinnamic acid (3-BrCA). For



pure 3-CICA, two polymorphs are known, corresponding to β -type (Kanao *et al.*, 1990) and γ -type (Kariuki *et al.*, 1996) structures. For pure 3-BrCA, two polymorphs are also known, again corresponding to β -type (Kanao *et al.*, 1990) and γ -type (Ahn *et al.*, 2001) structures. The γ -type polymorphs of 3-CICA and 3-BrCA are isostructural, whereas the β -type polymorphs of 3-CICA and 3-BrCA are structurally distinct.



A previous study reported (Ahn *et al.*, 2001) that the γ polymorph of 3-BrCA undergoes a polymorphic transformation to the β polymorph on heating above 373 K. In the present article, we investigate the possibility that a phase transformation may also occur for the γ polymorph of 3-CICA. Polymorphic phase transformations (Taylor *et al.*, 2014; Khoj *et al.*, 2013; Yates & Sparkes, 2013; Palmer *et al.*, 2012; Pete *et al.*, 2015; Rubin-Preminger *et al.*, 2004; Sørensen & Simonsen, 1989; Das *et al.*, 2010; Hu & Englert, 2005; Zhang *et al.*, 2005; Ahn *et al.*, 2006; Williams *et al.*, 2012) represent a ‘tipping point’ at which a gradual change in conditions (*e.g.* temperature) leads to the sudden conversion of one crystalline material into another (Dunitz, 1991; Meijer *et al.*, 2003).

Such processes are often accompanied by loss of crystallinity, with a single crystal of the starting phase transforming to a polycrystalline sample of the product phase. In some cases, however, particularly if the rearrangement involves only relatively minor atomic or molecular movements, a single crystal of the starting material may transform to a single crystal of the product. On rare occasions, reversible single-crystal to single-crystal transformations may be observed (Rubin-Preminger *et al.*, 2004; Sørensen & Simonsen, 1989; Das *et al.*, 2010; Hu & Englert, 2005; Zhang *et al.*, 2005; Pete *et al.*, 2015).

The formation of solid solutions composed of mixtures of *trans*-cinnamic acid derivatives has been reported previously (Hung *et al.*, 1972) and it has been shown (Khoj *et al.*, 2017) that, for a given binary system, solid solutions with a range of diverse structures can be formed depending on the composition of the material. In the case of solid solutions containing 3-CICA and 3-BrCA [such solid solutions are denoted 3-(Cl/Br)CA], two different β -type structures and two different γ -type structures have been reported (Khoj *et al.*, 2017). One of the β -type structures [denoted $\beta^{(Cl)}$] of the 3-(Cl/Br)CA solid solutions is structurally similar to the β polymorph of pure 3-CICA, whereas the other β -type structure [denoted $\beta^{(Br)}$] of the 3-(Cl/Br)CA solid solutions is structurally similar to the β polymorph of pure 3-BrCA. One of the γ -type structures (denoted γ) of the 3-(Cl/Br)CA solid

solutions is isostructural with the γ polymorphs of pure 3-CICA and pure 3-BrCA, whereas the other γ -type structure (denoted γ') of the 3-(Cl/Br)CA solid solutions has not been observed for either of the pure components. For 3-(Cl/Br)CA solid solutions prepared by crystallization from molten mixtures of 3-CICA and 3-BrCA, the structure type of the 3-(Cl/Br)CA solid solution has been found to depend on the relative amounts of the two components in the molten phase. The $\beta^{(Cl)}$ polymorph is obtained when the mole fraction of 3-CICA is in the range $x_{Cl} = 0.75$ –1 and the $\beta^{(Br)}$ polymorph is obtained when the mole fraction of 3-CICA is in the range $x_{Cl} = 0$ –0.67 (the intermediate region of $x_{Cl} = 0.67$ –0.75 has yet to be explored). The present article includes an investigation of a polymorphic phase transformation for a 3-(Cl/Br)CA solid solution prepared from a mixture with a molar ratio of 1:1 ($x_{Cl} \approx 0.5$).

2. Experimental

2.1. Crystallization

Samples of 3-CICA and 3-BrCA used in the present work were obtained from Alfa Aesar and solvents were obtained from Fisher. Crystallization was carried out by dissolution in an appropriate solvent and slow evaporation at ambient temperature. The γ polymorph of 3-CICA was obtained by crystallization from methanol and the γ polymorph of 3-BrCA was used as purchased. The polymorphic identity of each material was confirmed by powder XRD.

The 3-(Cl/Br)CA solid solution was prepared by crystallization from a solution containing 3-CICA and 3-BrCA in a 1:1 molar ratio dissolved in methanol. The powder XRD pattern of the material recovered from the crystallization is similar to the powder XRD patterns of the γ polymorphs of pure 3-CICA and pure 3-BrCA, which are isostructural. Thus, the solid solution is identified as the γ -type structure of 3-(Cl/Br)CA. Crystal structure determinations carried out previously (Khoj *et al.*, 2017) and in this work show that the composition of the 3-(Cl/Br)CA solid solution prepared by this method is approximately $(3\text{-CICA})_{0.57}(3\text{-BrCA})_{0.43}$, and thus contains an excess of 3-CICA relative to the composition of the crystallization solution.

2.2. Powder XRD

Powder XRD data were recorded at ambient temperature on a Bruker D8 instrument operating in transmission mode (Ge-monochromated Cu $K\alpha_1$ radiation). Samples were ground and sandwiched between pieces of transparent tape (foil-type sample holder).

2.3. Thermal analysis

Differential scanning calorimetry (DSC) was carried out on a TA Instruments Q100 DSC instrument. The sample (*ca* 2–4 mg) was placed in a hermetically sealed pan. Heating and cooling cycles were carried out at 20 K min^{-1} with an equilibration time of 1 min between heating and cooling cycles.

Table 1

Crystallographic data for the γ -type and $\beta^{(\text{Br})}$ -type structures of the 3-(Cl/Br)CA solid solution determined before and after the phase transformation from the γ -type structure to the $\beta^{(\text{Br})}$ -type structure.

Compound	3-(Cl _{0.57} /Br _{0.43})CA	3-(Cl _{0.51} /Br _{0.49})CA
Polymorph	γ	$\beta^{(\text{Br})}$
M_r	201.49	204.38
T (K)	296 (2)	296 (2)
Crystal system	Monoclinic	Monoclinic
Space group	$P2_1/a$	$C2/c$
a (Å)	12.3957 (8)	19.054 (5)
b (Å)	4.9381 (2)	3.9451 (7)
c (Å)	14.2102 (12)	24.661 (5)
α (°)	90	90
β (°)	94.871 (6)	111.81 (3)
γ (°)	90	90
V (Å ³)	866.68 (10)	1721.1 (7)
Z	4	8
Wavelength (Å)	1.54184	1.54184
ρ (calc) (Mg m ⁻³)	1.544	1.578
μ (mm ⁻¹)	4.627	4.828
Occupancies 3-CICA/3-BrCA	0.575 (4)/0.425 (4)	0.506 (7)/0.494 (7)
Crystal size (mm)	0.289 × 0.098 × 0.048	0.185 × 0.052 × 0.043
Reflections collected	2874	5012
Independent reflections	1670	1706
R_{int}	0.0440	0.0522
$R1$ [$I > 2\sigma(I)$]	0.0367	0.0494
$wR2$ [$I > 2\sigma(I)$]	0.0899	0.1308
$R1$ (all data)	0.0479	0.0763
$wR2$ (all data)	0.0972	0.1516

Computer programs: *CrysAlis PRO* (Rigaku OD, 2015) and *SHELXS2013* (Sheldrick, 2015a), *SHELXL2013* (Sheldrick, 2015b) and *Mercury* (Macrae et al., 2008).

2.4. Crystal structure determination

Crystal data, data collection and structure refinement details are summarized in Table 1. Single-crystal XRD data were recorded at ambient temperature using an Agilent SuperNova Dual Atlas diffractometer [mirror monochromator and Cu $K\alpha$ ($\lambda = 1.54180$ Å) radiation]. H atoms were inserted in idealized positions and refined using a riding model, with $U_{\text{iso}}(\text{H})$ values equal to 1.2 or 1.5 times the U_{eq} value of the atom to which it is bonded. Initial refinement with the halogen site occupied by only Cl or only Br showed unusually small or large displacement parameters. An additional electron-density peak from the difference map was then assigned as the other halogen and both C–X distances and displacement parameters were restrained. For the 3-(Cl/Br)CA solid solution, the fractional occupancies of the halogens

Table 2

Crystallographic data for the β and γ polymorphs of pure 3-CICA and pure 3-BrCA reported in previous publications.

Compound	3-CICA	3-BrCA	3-CICA	3-BrCA
Polymorph	γ	γ	β	β
Reference	Kariuki et al. (1996)	Ahn et al. (2001)	Kanao et al. (1990)	Kanao et al. (1990)
T (K)	293	293	295	295
Space group	$P2_1/a$	$P2_1/a$	$P\bar{1}$	$C2/c$
a (Å)	12.400 (1)	12.389 (2)	8.618 (4)	19.191 (6)
b (Å)	4.9560 (4)	4.933 (5)	13.627 (5)	3.9879 (3)
c (Å)	13.943 (1)	14.411 (2)	3.909 (1)	24.798 (7)
α (°)	90	90	106.77 (3)	90
β (°)	94.265 (3)	95.426 (5)	96.26 (3)	113.05 (2)
γ (°)	90	90	75.71 (3)	90
V (Å ³)	854.486	876.781	425.586	1746.319

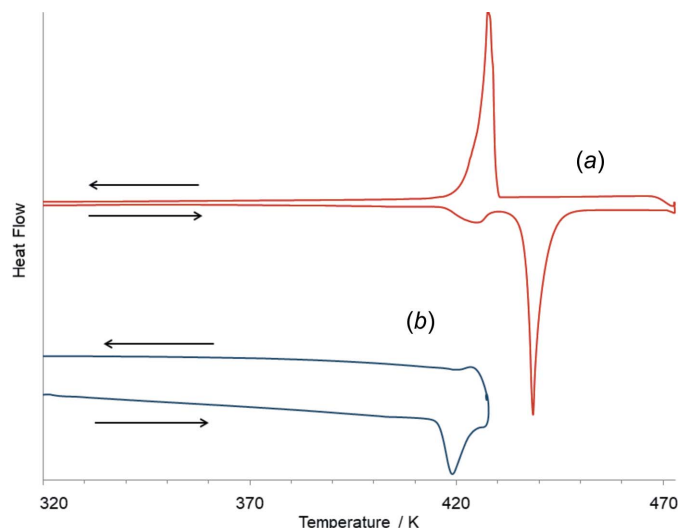


Figure 1 DSC data recorded on heating and cooling, starting from the γ polymorph of 3-CICA, showing (a) the heating-cooling cycle involving the polymorphic transformation, melting and recrystallization, and (b) the heating-cooling cycle involving only the polymorphic transformation.

occupying the site were constrained to a total occupancy of unity.

3. Results and discussion

3.1. Phase transformation of the γ polymorph of 3-CICA

DSC data (Fig. 1a) were recorded on heating the γ polymorph of 3-CICA from ambient temperature to 473 K and for the subsequent cooling cycle. In the heating cycle, two endotherms are observed (onset temperatures of ca 416 and 436 K); in the cooling cycle, only one exotherm is observed (ca 430 K). The thermal event at 436 K on heating is due to melting and the event at 430 K in the cooling cycle is due to crystallization.

To understand the thermal event at 416 K on heating, a DSC measurement (Fig. 1b) was carried out in which the γ polymorph of 3-CICA was heated from 313 to 428 K (*i.e.* below the melting temperature), then cooled to ambient temperature. In this case, no exotherm is observed in the cooling cycle, indicating that the endothermic process at 416 K on heating is irreversible. Powder XRD data confirmed that

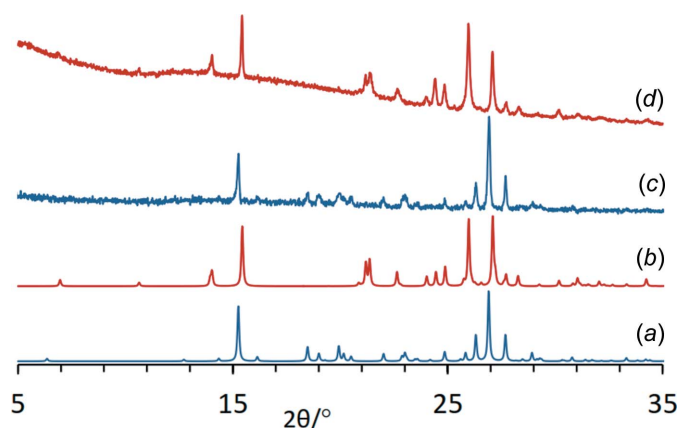


Figure 2
Powder XRD data calculated for the known crystal structures of (a) the γ polymorph of 3-CICA and (b) the β polymorph of 3-CICA. Experimental powder XRD patterns recorded for (c) the γ polymorph of 3-CICA and (d) the product obtained following the irreversible phase transformation that occurs on heating the γ polymorph of 3-CICA.

the sample recovered from this DSC experiment is the β polymorph of 3-CICA (Figs. 2b and 2d). Thus, the thermal event at 416 K on heating is assigned as a polymorphic transformation from the γ polymorph to the β polymorph of

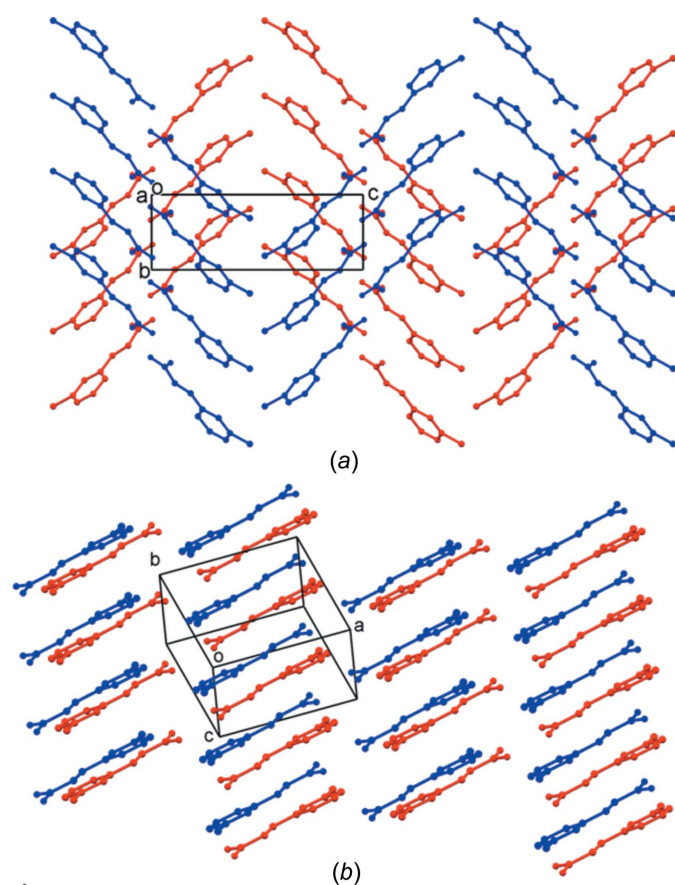


Figure 3
The crystal structures of (a) the γ polymorph of 3-CICA and (b) the β polymorph of 3-CICA. In each case, two adjacent layers in the crystal structure are shown, with one layer in red and the other layer in blue, and H atoms have been omitted for clarity. Each layer comprises stacks of hydrogen-bonded pairs of molecules.

3-CICA, with the β polymorph remaining as the stable polymorph on cooling to ambient temperature.

In the transformation from the γ polymorph to the β polymorph of 3-CICA, the molecular conformation remains as the *anti* conformation (see Scheme 1), but the polymorphic transformation is associated with substantial structural reorganization (see Table 2) from a herringbone arrangement in the γ polymorph (Fig. 3a) to a parallel arrangement in the β polymorph (Fig. 3b).

An analogous phase transformation has been reported (Ahn *et al.*, 2001) for 3-BrCA, with the γ polymorph transforming to the β polymorph on heating above 373 K. In the present work, DSC results starting from the γ polymorph of 3-BrCA showed evidence for a transformation at *ca* 418 K on heating. The transformation from the γ polymorph to the β polymorph again involves significant structural rearrangement [similar to that illustrated in Fig. 4 for the 3-(Cl/Br)CA solid solution, which is discussed in the next section], which in this case involves a change in molecular conformation from *anti* in the γ polymorph to *syn* in the β polymorph.

It is noteworthy that, although the γ polymorphs of 3-CICA and 3-BrCA are isostructural, the high-temperature polymorphic transformations in these materials produce β -type structures that are substantially different from each other.

3.2. Phase transformation in a 3-(Cl/Br)CA solid solution

The formation of solid solutions containing 3-CICA and 3-BrCA has been reported recently (Khoj *et al.*, 2017). In the

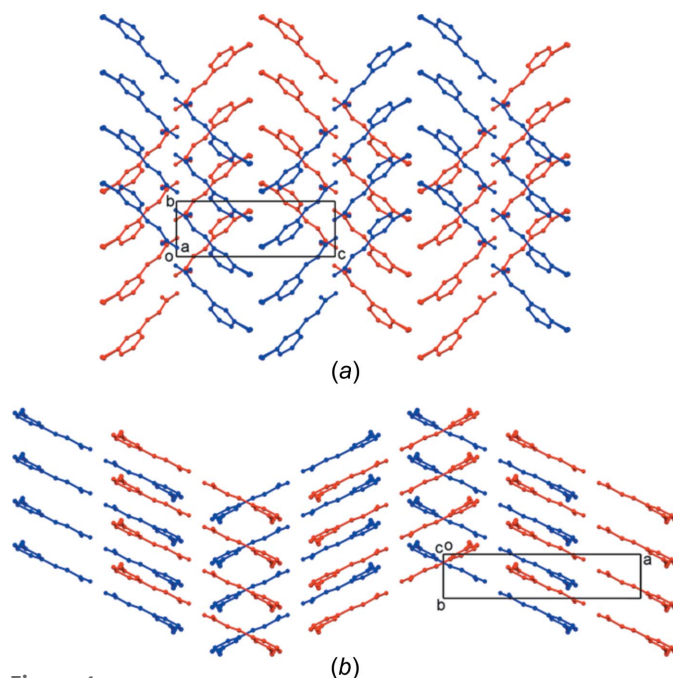


Figure 4
The crystal structures of (a) the γ polymorph of the 3-(Cl/Br)CA solid solution and (b) the $\beta^{(Br)}$ polymorph of the 3-(Cl/Br)CA solid solution. In each case, adjacent layers in the crystal structure are shown, with one layer in red and the other layer in blue, and H atoms have been omitted for clarity. Each layer comprises stacks of hydrogen-bonded pairs of molecules.

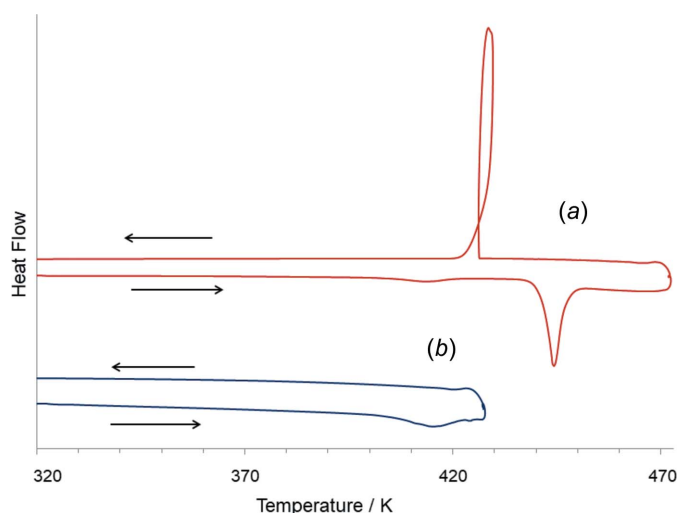


Figure 5 DSC data recorded for the γ polymorph of the 3-(Cl/Br)CA solid solution, showing (a) the heating-cooling cycle involving the polymorphic transformation, melting and recrystallization, and (b) the heating-cooling cycle involving only the polymorphic transformation. The loop in the cooling cycle is due to supercooling. Supercooling occurs on cooling the sample from the melt and the subsequent sudden release of energy on crystallization leads to a temperature rise in the sample and hence the loop observed (Anestiev & Malakhov, 2006).

present work, a 3-(Cl/Br)CA solid solution with the γ -type structure was obtained by crystallization from a solution containing 3-CICA and 3-BrCA in a 1:1 molar ratio dissolved in methanol.

From single-crystal XRD, the composition of a crystal selected from this sample was determined to be $(3\text{-CICA})_{0.57}(3\text{-BrCA})_{0.43}$ (Table 1), in close agreement with the results reported (Khoj *et al.*, 2017) recently for a crystal prepared by the same procedure [for which the composition was $(3\text{-CICA})_{0.56}(3\text{-BrCA})_{0.44}$]. The γ -type structure of the 3-(Cl/Br)CA solid solution is isostructural with the γ polymorphs of the pure end-members 3-CICA and 3-BrCA. The peak positions in the powder XRD data recorded for the γ -type structure of the 3-(Cl/Br)CA solid solution indicate that the unit-cell parameters are intermediate between those of the γ polymorphs of pure 3-CICA and pure 3-BrCA.

In the light of the polymorphic transformations observed on heating the γ polymorphs of pure 3-CICA and pure 3-BrCA, it is relevant to investigate whether the γ -type structure of the 3-(Cl/Br)CA solid solution also undergoes a phase transformation at elevated temperature, and if so, to establish whether the structure formed is analogous to the β -type structure of pure 3-CICA or to the β -type structure of pure 3-BrCA. DSC data (Fig. 5a) recorded on heating the γ -type structure of the 3-(Cl/Br)CA solid solution reveals an endotherm at *ca* 413 K and a symmetric endotherm (representing melting) at *ca* 437 K. The symmetric melting peak observed is consistent with the sample being a monophasic solid solution, rather than a physical mixture of pure 3-CICA and pure 3-BrCA (which may be expected to show an asymmetric melting peak). For the cooling cycle, an exotherm at *ca* 426 K arises due to crystallization. Further DSC data (Fig. 5b), recorded on

heating the sample to 428 K (below the melting temperature) followed by cooling, show that the polymorphic transformation is irreversible. Powder XRD data (Fig. 6) recorded for the material recovered from each DSC experiment resembles the powder XRD pattern of the β polymorph of 3-BrCA in each case, thus confirming the assignment of the product from the phase transformation as the $\beta^{(\text{Br})}$ structure type of the 3-(Cl/Br)CA solid solution.

The phase transformation has also been confirmed by single-crystal XRD, with the same crystal used for structure determination before and after heating (Table 1). A preliminary investigation revealed that a significant amount of sublimation occurred when the crystal was held at a high temperature for an extended period of time, as required to carry out the phase transformation and to complete the single-crystal XRD data collection at the same temperature. For this reason, the phase transformation was carried out *ex situ* by placing the crystal on a glass slide at 418 K for *ca* 90 s, before carrying out a single-crystal XRD data collection at low temperature (293 K) on the crystal following the phase transformation. The crystal size decreased to around one-third of the original size as a consequence of sublimation, and it is noteworthy that the 3-CICA and 3-BrCA molar ratio in the crystal changed from $(3\text{-CICA})_{0.57}(3\text{-BrCA})_{0.43}$ in the γ -type structure before the transformation to $(3\text{-CICA})_{0.51}(3\text{-BrCA})_{0.49}$ in the $\beta^{(\text{Br})}$ -type structure after the transformation, indicating preferential loss of 3-CICA through sublimation. Although it is clear from this single-crystal XRD study that the γ -type structure of the 3-(Cl/Br)CA solid solution transforms to the $\beta^{(\text{Br})}$ structure type in this high-temperature phase transformation and remains as the $\beta^{(\text{Br})}$ structure type on returning to ambient temperature, mechanistic details of the phase transformation remain to be understood as it is unclear at this stage

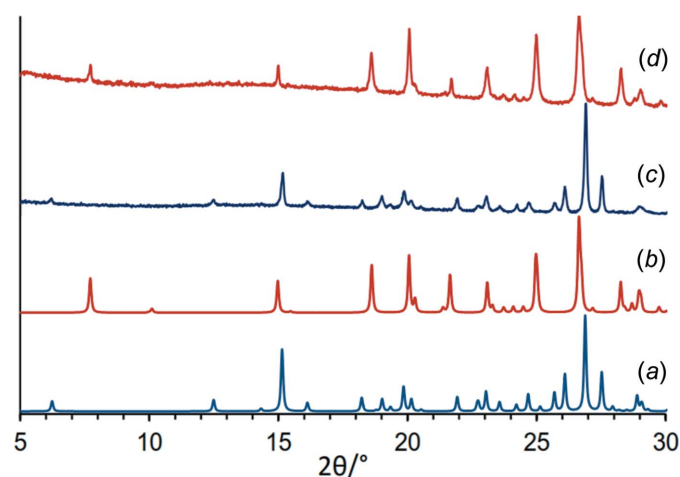


Figure 6 Powder XRD data calculated for the crystal structures of (a) the γ -type structure of the 3-(Cl/Br)CA solid solution and (b) the $\beta^{(\text{Br})}$ -type structure of the 3-(Cl/Br)CA solid solution. Crystallographic data for these structures are given in Table 1. Experimental powder XRD patterns recorded for (c) the γ -type structure of the 3-(Cl/Br)CA solid solution and (d) the product obtained following the irreversible phase transformation that occurs on heating the γ -type structure of the 3-(Cl/Br)CA solid solution.

whether the partial sublimation of the original crystal plays any role in the phase transformation mechanism.

4. Concluding remarks

For both pure 3-ClCA and pure 3-BrCA, an irreversible transformation from the γ polymorph to the β polymorph occurs in a similar temperature region (*ca* 416 and 418 K, respectively), which is also close to the temperature (413 K) of an irreversible transformation observed for the 3-(Cl/Br)CA solid solution with a molar ratio close to 1:1. These observations suggest that the γ polymorphs of 3-ClCA, 3-BrCA and 3-(Cl/Br)CA are metastable relative to the corresponding β polymorphs across the temperature range investigated. In each case, the polymorphic transformation involves considerable structural reorganization (see Figs. 3 and 4).

Although the γ polymorph of pure 3-ClCA is isostructural with the γ polymorph of pure 3-BrCA, the structure of the β polymorph produced in the polymorphic transformation for 3-ClCA is *different* from the structure of the β polymorph obtained in the corresponding transformation for 3-BrCA. The γ -type structure of the 3-(Cl/Br)CA solid solution is isostructural with the γ polymorphs of pure 3-ClCA and pure 3-BrCA. On heating the γ polymorph of the 3-(Cl/Br)CA solid solution, the $\beta^{(\text{Br})}$ structure obtained following the phase transformation is structurally similar to the β polymorph of pure 3-BrCA (rather than the β polymorph of pure 3-ClCA). The effect of varying the composition of the 3-(Cl/Br)CA solid solution on the polymorphic transformation and, in particular, the effect of composition on the structure type of the product phase obtained will be the focus of future research.

Acknowledgements

We thank Umm Al-Qura University, the Kingdom of Saudi Arabia (MAK) and Cardiff University for financial and material support.

References

Ahn, S., Guo, F., Kariuki, B. M. & Harris, K. D. M. (2006). *J. Am. Chem. Soc.* **128**, 8441–8452.
 Ahn, S., Harris, K. D. M., Kariuki, B. M. & Zin, D. M. S. (2001). *J. Solid State Chem.* **156**, 10–15.
 Anestiev, L. & Malakhov, D. (2006). *J. Non-Cryst. Solids*, **352**, 3350–3355.
 Cohen, M. D. (1964). *Pure Appl. Chem.* **9**, 567–574.
 Cohen, M. D. (1975). *Angew. Chem.* **87**, 439–447.
 Cohen, M. D. & Schmidt, G. M. J. (1964). *J. Chem. Soc.* pp. 1996–2000.
 Cohen, M. D., Schmidt, G. M. J. & Sonntag, F. I. (1964). *J. Chem. Soc.* pp. 2000–2013.

Das, D., Engel, E. & Barbour, L. J. (2010). *Chem. Commun.* **46**, 1676–1678.
 Dunitz, J. D. (1991). *Pure Appl. Chem.* **63**, 177–185.
 Enkelmann, V., Wegner, G., Novak, K. & Wagener, K. B. (1993). *J. Am. Chem. Soc.* **115**, 10390–10391.
 Guo, F., Martí-Rujas, J., Pan, Z., Hughes, C. E. & Harris, K. D. M. (2008). *J. Phys. Chem. C*, **112**, 19793–19796.
 Harris, K. D. M., Thomas, J. M. & Williams, D. (1991). *J. Chem. Soc. Faraday Trans.* **87**, 325–331.
 Hasegawa, M. (1986). *Pure Appl. Chem.* **58**, 1179–1188.
 Hirshfield, F. L. & Schmidt, G. M. J. (1964). *J. Polym. Sci. A Gen. Pap.* **2**, 2181–2190.
 Hu, C. & Englert, U. (2005). *Angew. Chem. Int. Ed.* **44**, 2281–2283.
 Hung, J. D., Lahav, M., Luwisch, M. & Schmidt, G. M. J. (1972). *Isr. J. Chem.* **10**, 585–599.
 Kanao, S., Kashino, S. & Haisa, M. (1990). *Acta Cryst.* **C46**, 2436–2438.
 Kariuki, B. M., Zin, D. M. S., Tremayne, M. & Harris, K. D. M. (1996). *Chem. Mater.* **8**, 565–569.
 Khoj, M. A., Hughes, C. E., Harris, K. D. M. & Kariuki, B. M. (2013). *Cryst. Growth Des.* **13**, 4110–4117.
 Khoj, M. A., Hughes, C. E., Harris, K. D. M. & Kariuki, B. M. (2017). *Cryst. Growth Des.* **17**, 1276–1284.
 Kohlschütter, V. & Tüscher, J. L. (1920). *Z. Anorg. Allg. Chem.* **111**, 193–236.
 Macrae, C. F., Bruno, I. J., Chisholm, J. A., Edgington, P. R., McCabe, P., Pidcock, E., Rodriguez-Monge, L., Taylor, R., van de Streek, J. & Wood, P. A. (2008). *J. Appl. Cryst.* **41**, 466–470.
 Meijer, M. D., Gebbink, R. J. M. K. & Van Koten, G. (2003). *Perspect. Supramol. Chem.* **7**, 375–386.
 Mustafa, A. (1952). *Chem. Rev.* **51**, 1–23.
 Nakanishi, H., Jones, W., Thomas, J. M., Hursthouse, M. B. & Motevalli, M. (1981). *J. Phys. Chem.* **85**, 3636–3642.
 Palmer, B. A., Kariuki, B. M., Morte-Ródenas, A. & Harris, K. D. M. (2012). *Cryst. Growth Des.* **12**, 577–582.
 Pete, U. D., Dikundwar, A. G., Sharma, V. M., Gejji, S. P., Bendre, R. S. & Guru Row, T. N. (2015). *CrystEngComm*, **17**, 7482–7485.
 Rigaku OD (2015). *CrysAlis PRO*. Rigaku Oxford Diffraction Ltd, Yarnton, Oxfordshire, England.
 Rubin-Preminger, J. M., Bernstein, J., Harris, R. K., Evans, I. R. & Ghi, P. Y. (2004). *J. Pharm. Sci.* **93**, 2810–2819.
 Schmidt, G. M. J. (1964). *J. Chem. Soc.* pp. 2014–2021.
 Schmidt, G. M. J. (1967). *Reactivity of the Photoexcited Molecule*, pp. 227–284. New York: Interscience.
 Schmidt, G. M. J. (1971). *Pure Appl. Chem.* **27**, 647–678.
 Sheldrick, G. M. (2015). *Acta Cryst.* **C71**, 3–8.
 Sørensen, A. M. & Simonsen, O. (1989). *Acta Cryst.* **C45**, 506–509.
 Taylor, R. G. D., Yeo, B. R., Hallett, A. J., Kariuki, B. M. & Pope, S. J. A. (2014). *CrystEngComm*, **16**, 4641–4652.
 Thomas, J. M. (1974). *Trans. R. Soc. A*, **277**, 251–286.
 Thomas, J. M. (1979). *Pure Appl. Chem.* **51**, 1065–1082.
 Williams, P. A., Hughes, C. E., Lim, G. K., Kariuki, B. M. & Harris, K. D. M. (2012). *Cryst. Growth Des.* **12**, 3104–3113.
 Yates, J. L. R. & Sparkes, H. A. (2013). *CrystEngComm*, **15**, 3547–3557.
 Zhang, J.-P., Lin, Y.-Y., Zhang, W.-X. & Chen, X.-M. (2005). *J. Am. Chem. Soc.* **127**, 14162–14163.

supporting information

Acta Cryst. (2018). C74 [https://doi.org/10.1107/S2053229618009269]

Polymorphic phase transformations of 3-chloro-*trans*-cinnamic acid and its solid solution with 3-bromo-*trans*-cinnamic acid

Manal A. Khoj, Colan E. Hughes, Kenneth D. M. Harris and Benson M. Kariuki

Computing details

For both structures, data collection: *CrysAlis PRO* (Rigaku OD, 2015); cell refinement: *CrysAlis PRO* (Rigaku OD, 2015); data reduction: *CrysAlis PRO* (Rigaku OD, 2015); program(s) used to solve structure: *SHELXS2013* (Sheldrick, 2015a); program(s) used to refine structure: *SHELXL2013* (Sheldrick, 2015b); software used to prepare material for publication: *SHELXL2013* (Sheldrick, 2015b).

3-(3-Chloro/bromophenyl)prop-2-enoic acid (I)

Crystal data

$C_9H_7Br_{0.43}Cl_{0.57}O_2$
 $M_r = 201.49$
 Monoclinic, $P2_1/a$
 $a = 12.3957$ (8) Å
 $b = 4.9381$ (2) Å
 $c = 14.2102$ (12) Å
 $\beta = 94.871$ (6)°
 $V = 866.68$ (10) Å³
 $Z = 4$

$F(000) = 405$
 $D_x = 1.540$ Mg m⁻³
 Cu $K\alpha$ radiation, $\lambda = 1.54184$ Å
 Cell parameters from 1154 reflections
 $\theta = 6.2\text{--}72.3^\circ$
 $\mu = 4.63$ mm⁻¹
 $T = 296$ K
 Needle, colourless
 0.29 × 0.10 × 0.05 mm

Data collection

Agilent SuperNova Dual Source
 diffractometer with an Atlas detector
 ω scans
 Absorption correction: gaussian
 (CrysAlis PRO; Rigaku OD, 2015)
 $T_{\min} = 0.893$, $T_{\max} = 0.969$
 2874 measured reflections

1670 independent reflections
 1306 reflections with $I > 2\sigma(I)$
 $R_{\text{int}} = 0.044$
 $\theta_{\max} = 73.9^\circ$, $\theta_{\min} = 6.3^\circ$
 $h = -14 \rightarrow 15$
 $k = -4 \rightarrow 5$
 $l = -17 \rightarrow 15$

Refinement

Refinement on F^2
 Least-squares matrix: full
 $R[F^2 > 2\sigma(F^2)] = 0.037$
 $wR(F^2) = 0.097$
 $S = 1.00$
 1670 reflections
 123 parameters
 20 restraints

Hydrogen site location: mixed
 H atoms treated by a mixture of independent
 and constrained refinement
 $w = 1/[\sigma^2(F_o^2) + (0.058P)^2]$
 where $P = (F_o^2 + 2F_c^2)/3$
 $(\Delta/\sigma)_{\max} < 0.001$
 $\Delta\rho_{\max} = 0.26$ e Å⁻³
 $\Delta\rho_{\min} = -0.34$ e Å⁻³

Special details

Geometry. All esds (except the esd in the dihedral angle between two l.s. planes) are estimated using the full covariance matrix. The cell esds are taken into account individually in the estimation of esds in distances, angles and torsion angles; correlations between esds in cell parameters are only used when they are defined by crystal symmetry. An approximate (isotropic) treatment of cell esds is used for estimating esds involving l.s. planes.

Fractional atomic coordinates and isotropic or equivalent isotropic displacement parameters (\AA^2)

	x	y	z	$U_{\text{iso}}^*/U_{\text{eq}}$	Occ. (<1)
C1	0.67233 (18)	-0.6465 (4)	0.23649 (16)	0.0493 (5)	
C2	0.62396 (18)	-0.5315 (5)	0.31173 (16)	0.0528 (5)	
H2	0.555859	-0.589481	0.325993	0.063*	
C3	0.6770 (2)	-0.3315 (5)	0.36513 (16)	0.0557 (6)	
C4	0.7783 (2)	-0.2403 (5)	0.34630 (19)	0.0610 (6)	
H4	0.813206	-0.105848	0.383226	0.073*	
C5	0.8267 (2)	-0.3534 (5)	0.27113 (19)	0.0629 (6)	
H5	0.894935	-0.294524	0.257509	0.075*	
C6	0.77456 (18)	-0.5532 (5)	0.21618 (17)	0.0552 (6)	
H6	0.807542	-0.625904	0.165490	0.066*	
C7	0.61382 (18)	-0.8594 (4)	0.18165 (17)	0.0510 (5)	
H7	0.546210	-0.906212	0.200428	0.061*	
C8	0.64617 (17)	-0.9925 (5)	0.10857 (15)	0.0513 (5)	
H8	0.712007	-0.946555	0.085987	0.062*	
C9	0.58153 (17)	-1.2110 (4)	0.06175 (16)	0.0471 (5)	
O1	0.62133 (13)	-1.3381 (3)	-0.00454 (13)	0.0589 (4)	
O2	0.48893 (13)	-1.2659 (4)	0.08900 (13)	0.0594 (5)	
Cl1	0.6164 (7)	-0.170 (2)	0.4567 (5)	0.0732 (12)	0.575 (4)
Br1	0.6053 (4)	-0.1842 (12)	0.4661 (2)	0.0710 (7)	0.425 (4)
H1O	0.438 (4)	-1.450 (11)	0.045 (3)	0.145 (16)*	

Atomic displacement parameters (\AA^2)

	U^{11}	U^{22}	U^{33}	U^{12}	U^{13}	U^{23}
C1	0.0526 (11)	0.0412 (11)	0.0539 (11)	-0.0002 (9)	0.0041 (9)	-0.0001 (9)
C2	0.0543 (11)	0.0489 (12)	0.0557 (11)	0.0021 (10)	0.0071 (9)	0.0010 (10)
C3	0.0681 (14)	0.0493 (12)	0.0498 (11)	0.0088 (11)	0.0064 (10)	-0.0025 (10)
C4	0.0654 (14)	0.0528 (13)	0.0634 (14)	-0.0014 (11)	-0.0032 (11)	-0.0090 (11)
C5	0.0553 (13)	0.0618 (15)	0.0716 (15)	-0.0067 (11)	0.0056 (11)	-0.0064 (12)
C6	0.0534 (12)	0.0523 (13)	0.0608 (13)	-0.0004 (10)	0.0096 (10)	-0.0089 (10)
C7	0.0493 (11)	0.0453 (11)	0.0588 (12)	-0.0021 (9)	0.0071 (9)	-0.0022 (10)
C8	0.0486 (10)	0.0474 (11)	0.0587 (12)	-0.0053 (9)	0.0090 (9)	-0.0025 (10)
C9	0.0470 (10)	0.0435 (10)	0.0512 (11)	0.0015 (9)	0.0071 (9)	-0.0011 (9)
O1	0.0573 (9)	0.0563 (10)	0.0656 (9)	-0.0072 (7)	0.0193 (7)	-0.0138 (8)
O2	0.0530 (9)	0.0614 (9)	0.0657 (10)	-0.0096 (7)	0.0167 (7)	-0.0126 (8)
Cl1	0.097 (2)	0.0690 (15)	0.0584 (15)	-0.0042 (11)	0.0339 (11)	-0.0167 (14)
Br1	0.0888 (13)	0.0720 (11)	0.0543 (8)	0.0109 (12)	0.0182 (9)	-0.0098 (7)

Geometric parameters (Å, °)

C1—C2	1.391 (3)	C5—C6	1.384 (3)
C1—C6	1.401 (3)	C5—H5	0.9300
C1—C7	1.464 (3)	C6—H6	0.9300
C2—C3	1.378 (3)	C7—C8	1.320 (3)
C2—H2	0.9300	C7—H7	0.9300
C3—C4	1.381 (4)	C8—C9	1.469 (3)
C3—C11	1.7504 (10)	C8—H8	0.9300
C3—Br1	1.896 (4)	C9—O1	1.266 (3)
C4—C5	1.387 (4)	C9—O2	1.271 (3)
C4—H4	0.9300	O2—H1O	1.24 (5)
C2—C1—C6	118.7 (2)	C6—C5—H5	119.7
C2—C1—C7	118.4 (2)	C4—C5—H5	119.7
C6—C1—C7	122.8 (2)	C5—C6—C1	120.4 (2)
C3—C2—C1	120.0 (2)	C5—C6—H6	119.8
C3—C2—H2	120.0	C1—C6—H6	119.8
C1—C2—H2	120.0	C8—C7—C1	127.4 (2)
C2—C3—C4	121.7 (2)	C8—C7—H7	116.3
C2—C3—C11	121.5 (4)	C1—C7—H7	116.3
C4—C3—C11	116.7 (4)	C7—C8—C9	122.11 (19)
C2—C3—Br1	117.3 (3)	C7—C8—H8	118.9
C4—C3—Br1	120.9 (3)	C9—C8—H8	118.9
C11—C3—Br1	4.9 (6)	O1—C9—O2	122.7 (2)
C3—C4—C5	118.6 (2)	O1—C9—C8	117.97 (18)
C3—C4—H4	120.7	O2—C9—C8	119.37 (19)
C5—C4—H4	120.7	C9—O2—H1O	115.5 (19)
C6—C5—C4	120.6 (2)		

3-(3-Chloro/bromophenyl)prop-2-enoic acid (II)

Crystal data

$C_9H_7Br_{0.49}Cl_{0.51}O_2$

$M_r = 204.38$

Monoclinic, $C2/c$

$a = 19.054 (5) \text{ \AA}$

$b = 3.9451 (7) \text{ \AA}$

$c = 24.661 (5) \text{ \AA}$

$\beta = 111.81 (3)^\circ$

$V = 1721.1 (7) \text{ \AA}^3$

$Z = 8$

$F(000) = 823$

$D_x = 1.578 \text{ Mg m}^{-3}$

Cu $K\alpha$ radiation, $\lambda = 1.54184 \text{ \AA}$

Cell parameters from 946 reflections

$\theta = 3.9\text{--}71.3^\circ$

$\mu = 4.83 \text{ mm}^{-1}$

$T = 296 \text{ K}$

Needle, colourless

$0.19 \times 0.05 \times 0.04 \text{ mm}$

Data collection

Agilent SuperNova Dual Source
diffractometer with an Atlas detector

ω scans

Absorption correction: gaussian
(CrysAlis PRO; Rigaku OD, 2015)

$T_{\min} = 0.961$, $T_{\max} = 0.987$

5012 measured reflections

1706 independent reflections

1181 reflections with $I > 2\sigma(I)$

$R_{\text{int}} = 0.052$

$\theta_{\max} = 74.4^\circ$, $\theta_{\min} = 3.9^\circ$

$h = -14 \rightarrow 23$

$k = -4 \rightarrow 4$

$l = -30 \rightarrow 26$

Refinement

Refinement on F^2
 Least-squares matrix: full
 $R[F^2 > 2\sigma(F^2)] = 0.049$
 $wR(F^2) = 0.152$
 $S = 1.03$
 1706 reflections
 120 parameters
 22 restraints

Hydrogen site location: inferred from neighbouring sites
 H-atom parameters constrained
 $w = 1/[\sigma^2(F_o^2) + (0.074P)^2 + 0.5938P]$
 where $P = (F_o^2 + 2F_c^2)/3$
 $(\Delta/\sigma)_{\max} < 0.001$
 $\Delta\rho_{\max} = 0.40 \text{ e } \text{\AA}^{-3}$
 $\Delta\rho_{\min} = -0.42 \text{ e } \text{\AA}^{-3}$

Special details

Geometry. All esds (except the esd in the dihedral angle between two l.s. planes) are estimated using the full covariance matrix. The cell esds are taken into account individually in the estimation of esds in distances, angles and torsion angles; correlations between esds in cell parameters are only used when they are defined by crystal symmetry. An approximate (isotropic) treatment of cell esds is used for estimating esds involving l.s. planes.

Fractional atomic coordinates and isotropic or equivalent isotropic displacement parameters (\AA^2)

	<i>x</i>	<i>y</i>	<i>z</i>	$U_{\text{iso}}^*/U_{\text{eq}}$	Occ. (<1)
C1	0.5351 (2)	0.6106 (11)	0.61622 (17)	0.0616 (10)	
C2	0.5504 (2)	0.5294 (10)	0.67517 (15)	0.0591 (9)	
H2	0.514805	0.579375	0.691554	0.071*	
C3	0.6161 (2)	0.3799 (10)	0.70801 (16)	0.0616 (9)	
C4	0.6709 (2)	0.2960 (10)	0.6851 (2)	0.0679 (10)	
H4	0.715608	0.188866	0.707907	0.081*	
C5	0.6565 (3)	0.3769 (13)	0.6280 (2)	0.0789 (13)	
H5	0.692530	0.326609	0.612053	0.095*	
C6	0.5904 (2)	0.5301 (13)	0.59378 (19)	0.0719 (11)	
H6	0.582205	0.581225	0.555083	0.086*	
C7	0.4650 (2)	0.7733 (10)	0.57900 (17)	0.0631 (10)	
H7	0.460976	0.822057	0.541064	0.076*	
C8	0.4064 (2)	0.8600 (11)	0.59242 (17)	0.0646 (10)	
H8	0.408265	0.812665	0.629870	0.078*	
C9	0.3394 (2)	1.0250 (12)	0.55188 (16)	0.0663 (10)	
Cl1	0.6387 (4)	0.293 (3)	0.7821 (3)	0.0674 (16)	0.506 (7)
Br1	0.6347 (3)	0.2667 (15)	0.78648 (14)	0.0824 (12)	0.494 (7)
O1	0.28940 (18)	1.1178 (10)	0.57129 (13)	0.0892 (11)	
H1	0.254247	1.207587	0.544981	0.134*	0.5
O2	0.33317 (19)	1.0789 (11)	0.49960 (12)	0.0858 (10)	
H2A	0.293100	1.176290	0.482034	0.129*	0.5

Atomic displacement parameters (\AA^2)

	U^{11}	U^{22}	U^{33}	U^{12}	U^{13}	U^{23}
C1	0.065 (2)	0.066 (2)	0.057 (2)	-0.0153 (18)	0.0263 (17)	-0.0109 (17)
C2	0.069 (2)	0.060 (2)	0.057 (2)	-0.0114 (17)	0.0325 (18)	-0.0071 (17)
C3	0.071 (2)	0.059 (2)	0.058 (2)	-0.0061 (18)	0.0291 (18)	-0.0015 (17)
C4	0.067 (2)	0.060 (2)	0.084 (3)	-0.0015 (18)	0.035 (2)	-0.0032 (19)
C5	0.076 (3)	0.091 (3)	0.085 (3)	-0.004 (2)	0.047 (2)	-0.012 (2)

C6	0.081 (3)	0.081 (3)	0.064 (2)	-0.014 (2)	0.039 (2)	-0.009 (2)
C7	0.077 (2)	0.064 (2)	0.052 (2)	-0.0116 (19)	0.0271 (18)	-0.0058 (17)
C8	0.076 (2)	0.068 (2)	0.051 (2)	-0.0069 (19)	0.0248 (18)	0.0009 (17)
C9	0.071 (2)	0.076 (3)	0.051 (2)	-0.011 (2)	0.0219 (18)	-0.0059 (19)
Cl1	0.065 (2)	0.073 (3)	0.062 (3)	-0.0005 (17)	0.020 (2)	0.020 (2)
Br1	0.106 (2)	0.086 (2)	0.0679 (12)	0.0151 (14)	0.0463 (12)	0.0122 (10)
O1	0.081 (2)	0.128 (3)	0.0655 (19)	0.013 (2)	0.0348 (16)	0.0167 (18)
O2	0.088 (2)	0.120 (3)	0.0515 (15)	0.0137 (19)	0.0292 (14)	0.0065 (16)

Geometric parameters (Å, °)

C1—C6	1.396 (6)	C5—H5	0.9300
C1—C2	1.410 (5)	C6—H6	0.9300
C1—C7	1.459 (6)	C7—C8	1.321 (6)
C2—C3	1.348 (6)	C7—H7	0.9300
C2—H2	0.9300	C8—C9	1.451 (6)
C3—C4	1.400 (6)	C8—H8	0.9300
C3—Cl1	1.748 (6)	C9—O2	1.268 (5)
C3—Br1	1.887 (5)	C9—O1	1.269 (5)
C4—C5	1.369 (7)	O1—H1	0.8200
C4—H4	0.9300	O2—H2A	0.8200
C5—C6	1.369 (7)		
C6—C1—C2	117.4 (4)	C4—C5—H5	119.2
C6—C1—C7	120.0 (4)	C6—C5—H5	119.2
C2—C1—C7	122.6 (4)	C5—C6—C1	120.9 (4)
C3—C2—C1	120.6 (3)	C5—C6—H6	119.6
C3—C2—H2	119.7	C1—C6—H6	119.6
C1—C2—H2	119.7	C8—C7—C1	128.1 (4)
C2—C3—C4	121.8 (4)	C8—C7—H7	115.9
C2—C3—Cl1	121.8 (4)	C1—C7—H7	115.9
C4—C3—Cl1	116.4 (4)	C7—C8—C9	123.5 (4)
C2—C3—Br1	119.9 (3)	C7—C8—H8	118.2
C4—C3—Br1	118.3 (4)	C9—C8—H8	118.2
Cl1—C3—Br1	3.8 (5)	O2—C9—O1	122.3 (4)
C5—C4—C3	117.8 (4)	O2—C9—C8	120.2 (4)
C5—C4—H4	121.1	O1—C9—C8	117.5 (3)
C3—C4—H4	121.1	C9—O1—H1	109.5
C4—C5—C6	121.6 (4)	C9—O2—H2A	109.5